M&C 2017 - International Conference on Mathematics & Computational Methods Applied to Nuclear Science & Engineering, Jeju, Korea, April 16-20, 2017, on USB (2017)

nTRACER and KENO V.a Calculations of the VENUS-9/1 Experimental Benchmark

Alexander Aures, Matías Zilly, Kiril Velkov, Winfried Zwermann

Gesellschaft für Anlagen- und Reaktorsicherheit (GRS) gGmbH, Boltzmannstraße 14, 85748 Garching, Germany
Alexander.Aures@grs.de

Han Gyu Joo

Department of Nuclear Engineering, Seoul National University, 599 Gwanak-ro, Gwanak-gu, Seoul 151-744, Korea
joohan@snu.ac.kr

Abstract – *Neutron transport calculations of the VENUS-9/1 experiment are performed with the deterministic code nTRACER and the Monte Carlo code KENO V.a from the SCALE 6.2 code package. The VENUS-9/1 experiment, documented in IRPhE project, was designed to analyse the power distribution across the boundary between an UO_2 fuel region and a MOX fuel region. Beside the nominal core configuration, three other core configurations were investigated, where seven UO_2 fuel rods next to the MOX fuel region were replaced by an aluminium plate, B_4C rods or water. The nTRACER and KENO V.a models represent the experiment in a simplified manner. Multiplication factors are compared between the neutron transport codes, and the calculated power distributions are compared to the experimental values. In terms of the multiplication factors, excellent agreement is found between nTRACER and KENO V.A in multi-group mode. Slightly larger deviations are obtained with KENO V.a in continuous-energy mode. Good agreement is found for the pin power distributions between the codes and the experiments. Larger discrepancies are only observed at the positions close to the boundary between the fuel regions and at the outer edge of the core.*

I. INTRODUCTION

Between 1967 and 1975, various critical experiments were performed at the zero power reactor VENUS (Vulcain Experimental Nuclear Study) at the Belgian research centre SCK/CEN in Mol. Among these experiments, the VENUS-9 and VENUS-9/1 configurations were carried out in 1967-1968. The main purpose of these experiments was the analysis of the power distribution across the boundary between a fresh UO_2 fuel region and a mixed oxide fuel (MOX) region, the latter representing fuel irradiated for one cycle. These configurations became part of the *International Handbook of Evaluated Reactor Physics Benchmark Experiments* (IRPhE) [1].

The VENUS-9/1 configuration was set up in order to analyse the power distributions in the presence of different perturbations in terms of the geometry and utilized materials. The VENUS-9/1 nominal case consists of a fully loaded core. In three perturbed configurations, seven UO_2 fuel pin positions at the boundary between the different fuel regions were replaced by other materials: i) an aluminium plate of 0.905 cm thickness, ii) B_4C rods, and iii) water cells. In order to allow criticality, especially in case of the perturbation with the absorber rods, the fissile region was extended by additional rows of UO_2 fuel rods. The fissile region was moreover surrounded by water, and criticality was achieved by adjusting the water level. In all configurations, the pin power distributions were measured along a traverse crossing the UO_2 fuel region and the MOX fuel region. [1][2]

The VENUS-9 and 9/1 configurations have already been subject of investigations; for example, 3D Monte Carlo calculations with MCNP using JEF2.2 and JEFF3.1, and 2D lattice calculations with CASMO-4 and APOLLO2-A are outlined in [5]. Furthermore, the VENUS-9 and 9/1 configurations are similar to the VENUS-7 experiment, which was already subject to an international OECD/NEA benchmark [6] and became also part of the IRPhE project.

In this study, the VENUS-9/1 configuration was simplified by neglecting all structures above the critical water level and, additionally, by neglecting the reactor vessel and placing the core in the middle of the moderator region. The three-dimensional deterministic neutron transport code nTRACER is used to assess the multiplication factors and the power distributions of the VENUS-9/1 nominal case and the perturbation cases. The same quantities are determined with the Monte Carlo code KENO V.a from the SCALE 6.2 code package. The multiplication factors are compared between the codes, and the power distributions are compared to the experimental values.

II. MODEL AND CALCULATION METHODS

In the following sections, the models and calculation methods are outlined.

1. The VENUS-9/1 model

The core of the VENUS-9/1 experiment consists of two adjacent rectangular regions of UO_2 fuel rods. One region contains UO_2 fuel rods with 4 wt.-% enriched U-235 (UO_2 4/0), the other region contains MOX fuel rods with 3 wt.-% U-235 and 1.25 wt.-% fissile Pu (MOX 3/1). In order to achieve criticality, rectangular regions with 9 rows each of UO_2 4/0 fuel rods are added to the shorter sides of the core.

The UO_2 4/0 rods have an outer diameter of 0.978 cm including a stainless steel cladding of 0.038 cm thickness. The MOX 3/1 rods have an outer diameter of 1.010 cm including a 0.025 cm thick cladding made from Incoloy. The demountable UO_2 fuel rods and MOX fuel rods (DEM) have an outer diameter of 0.978 cm, and the fuel is encased in an aluminium/stainless steel double cladding. All fuel rods have an active height of 50 cm and both ends are equipped with a reflector made of Plexiglas. The ends of the fuel rods consist of stainless steel (Lower Stop) and the positions of the rods are fixed by stainless steel grids at both ends (Lower Grid). The core is placed on a structure called Reactor Support. It has a thickness of 9.4 cm and is a homogeneous mixture of 8.1 vol.-% stainless steel and 91.9 vol.-% water. Below this structure, there is a volume of water with a height of 83.45 cm. A temperature of 293 K is set for all materials. Along the traverse of the demountable fuel rods, the pin power distribution was measured. [1][2]

Several simplifications are made to the models for the simulation. The fuel rods and all other structural materials are modelled only up to the critical water level; above a vacuum boundary condition is assumed. Furthermore, the reactor vessel is neglected and the core is surrounded by about 35.181 cm of water on each side. The differences in the multiplication factors resulting from the simplifications are determined in a comparative analysis. Fig. 1 provides a top view of the core layout and Fig. 2 shows a side view of the core and the structure below the core. As an example, the B_4C perturbation configuration is shown, in which seven UO_2 fuel rods are replaced by B_4C rods.

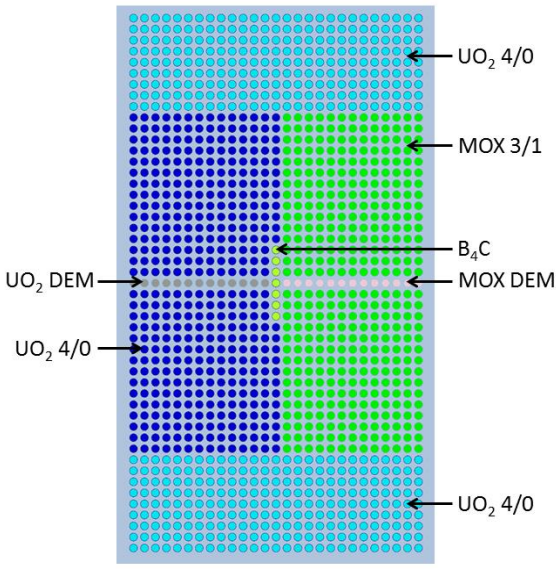

Fig. 1 Excerpt of the top view of the simplified VENUS-9/1 configuration, incl. the perturbation with seven B_4C rods.

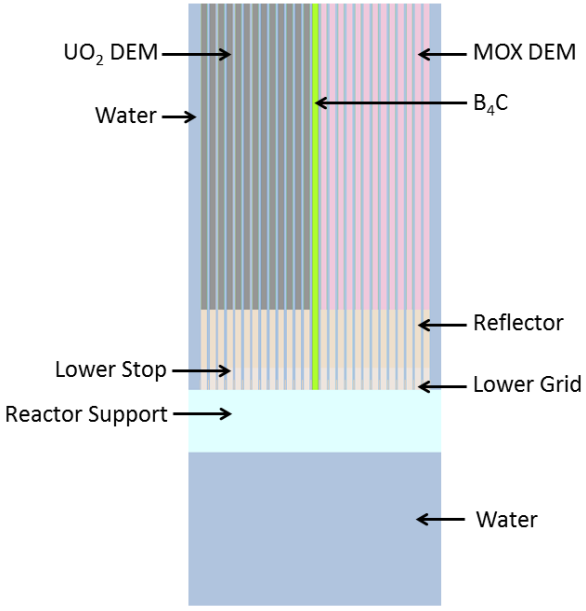

Fig. 2 Excerpt of the side view of the simplified VENUS-9/1 configuration, incl. the perturbation with seven B_4C rods.

2. Calculation methods

The neutron transport calculations are performed with the direct whole-core calculation code nTRACER [3] developed at the Seoul National University. nTRACER applies a planar MOC routine to solve a plane-wise 2D transport problem with sub-pin level details. The planes are coupled by a 3D CMFD calculation routine with an embedded SP_3 nodal method. By applying these routines iteratively, a 3D whole-core solution is obtained. The resonance treatment of the cross sections is done by application of the subgroup method [3]. The calculations are performed with a 47-group cross section library that is shipped with nTRACER. It is based on ENDF/B-VI data and adjusted to light water reactor systems.

For comparison, Monte Carlo calculations with KENO V.a of the SCALE 6.2 code package are performed. KENO V.a is primarily applied to determine multiplication factors and neutron flux distributions, and it can be used with continuous-energy (CE) or multi-group (MG) cross section data [4]. In this work, KENO calculations are performed in multi-group as well as continuous-energy

mode. The cross section libraries are based on the ENDF/B-VII.0 library, and in case of the multi-group calculation, the 238-group cross section library is applied. The calculations are performed with 8,000 neutron generations with 25,000 neutrons per generation. In addition to calculations with models as used in nTRACER, the influence of the applied simplifications is studied with KENO V.a.

III. RESULTS

This section outlines the results for the multiplication factors and the power distributions of the nominal and the perturbed VENUS-9/1 configurations.

1. Influence of the Modeling Simplifications

The VENUS-9/1 configuration is modelled with some simplifications, for example, fuel rods and all other structural materials above the critical water level are replaced with vacuum boundary conditions, and additionally, the core is surrounded by water only. In order to assess the impact of these simplifications, KENO V.a calculations in multi-group mode are performed with both the exact and simplified models. The reactivity difference is about -1700 pcm for the nominal case, the Al-plate perturbation case and the H_2O perturbation case. For the B_4C perturbation case, the simplification results in a difference of -1009 pcm.

2. Multiplication Factors

In Table I and II, multiplication factors determined with nTRACER and KENO V.a are compared for the nominal and perturbed VENUS-9/1 cases. Table I refers to the KENO V.a multi-group results and Table II lists the KENO V.a continuous-energy results. All multiplication factors calculated with KENO V.a have a relative error of 0.006 %. Although the individual measured critical water levels of the different configurations are adopted, the multiplication factors obtained by both transport codes are subcritical. The reason for this is the simplifications in terms of geometry and materials in the models (cf. Section III.1).

Table I Multiplication factors obtained from nTRACER and KENO V.a (238-group) of the nominal and perturbed VENUS-9/1 cases.

Case	nTRACER k_{eff}	KENO V.a MG k_{eff}	Δρ pcm
nominal	0.97900	0.97908	-8
Al-plate	0.97802	0.97786	17
B_4C	0.98574	0.98486	91
H_2O	0.97700	0.97712	-12

Table II Multiplication factors obtained from nTRACER and KENO V.a (continuous-energy) of the nominal and perturbed VENUS-9/1 cases.

Case	nTRACER k_{eff}	KENO V.a CE k_{eff}	Δρ pcm
nominal	0.97900	0.98001	-105
Al-plate	0.97802	0.97875	-77
B_4C	0.98574	0.98588	-15
H_2O	0.97700	0.97790	-95

Overall, the multiplication factors obtained by both transport codes are in very good agreement. In case of KENO V.a in multi-group mode, the smallest difference, -8 pcm, is observed for the nominal case, while the B_4C case shows the largest difference with 91 pcm. The opposite is observed for the application of KENO V.a in continuous-energy mode, namely, the smallest difference, -15 pcm, is obtained for the B_4C case and the largest difference, -105 pcm, is obtained for the nominal case. In combination with continuous-energy cross section data, KENO V.a determines larger multiplication factors than nTRACER for all cases, and additionally, larger reactivity differences are observed. The reactivity difference between KENO V.a continuous-energy and KENO V.a multi-group is about 100 pcm.

3. Power Distributions

Pin powers of the DEM fuel rods (cf. Fig. 1) obtained by nTRACER and KENO in multi-group and continuous-energy mode are compared to the experimental values given in the IRPhE documentation [1]. Since KENO MG and KENO CE show almost consistent results in all configurations, it will just be referred to "KENO" from this point onwards in the discussion of the pin power distributions.

Fig. 3 shows the pin power distribution of the nominal case. The positions -22 to -9 identify the UO_2 DEM rods, and the positions -8 to 4 identify the MOX DEM rods. The outermost pin positions of both fuel regions show a high power which is caused by the large amount of surrounding water. After a minimum at the positions -20 and 2, respectively, the pin power distribution in both fuel regions show an increase towards the middle of the core. At the boundary of the fuel regions, the UO_2 rods show a drop in the power, whereas the MOX rods experience an even larger increase in power.

In the middle of both fuel regions, all codes show good agreement with the experimental values. At the outer pin positions, nTRACER overestimates the power by about 5 % and at position -21 a relative deviation of about 10 % is observed. The pin powers calculated by KENO show good agreement at the outer UO_2 pins, but an underestimation of about -5 % is observed for the outer MOX pins. In the UO_2

fuel region, nTRACER underestimates the pin powers. The underestimation increases towards the middle of the core and reaches its maximum of about 5 % at position -9. On the contrary, KENO overestimates the power by about 2 %, however, it matches the experimental value at position -9. For the pin power at position -8, the first MOX rod next to the UO_2 fuel region, nTRACER and KENO agree well with the experimental value. This is also true for position -7. Moreover, the pin powers in the middle of the MOX region are slightly underestimated by all codes.

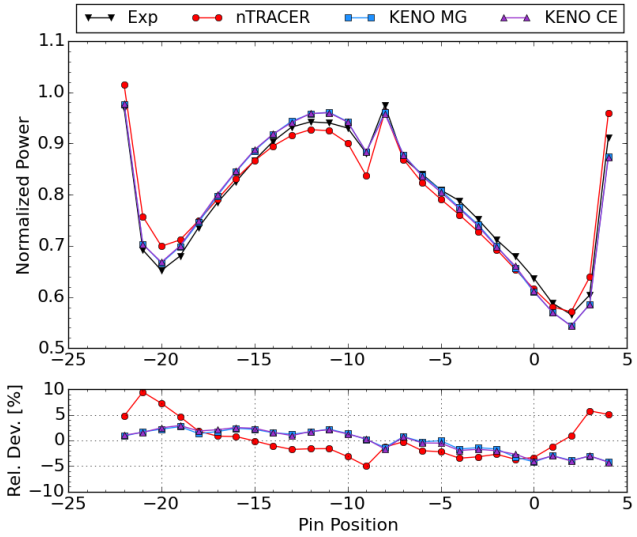

Fig. 3: Pin power distribution along the traverse of the VENUS-9/1 nominal case.

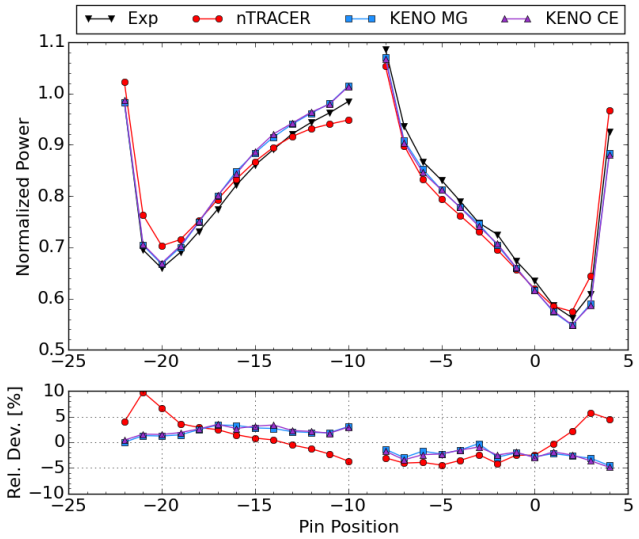

Fig. 4: Pin power distribution along the traverse of the VENUS-9/1 Al-plate perturbation case, where seven pin positions are replaced by an Al-plate at position -9.

In general, some trends can be observed: KENO shows an overestimation in the UO_2 region and an underestimation in the MOX region; nTRACER overstimates the pin power at the outer positions of both fuel regions and underestimates the pin power in the middle of the core.

In the perturbation cases described in the following, the UO_2 rods at position -9 are replaced. Fig. 4 shows the pin power distribution of the Al-plate perturbation case. Overall, the pin power distributions are similar to the ones of the nominal case. At the positions next to the perturbed cells, nTRACER underestimates the pin powers of the UO_2 rods by about 4 % and KENO underestimates the pin powers of about 3 %. Moreover, the perturbation leads to a slightly larger deviation between the calculated and experimental pin powers at position -8.

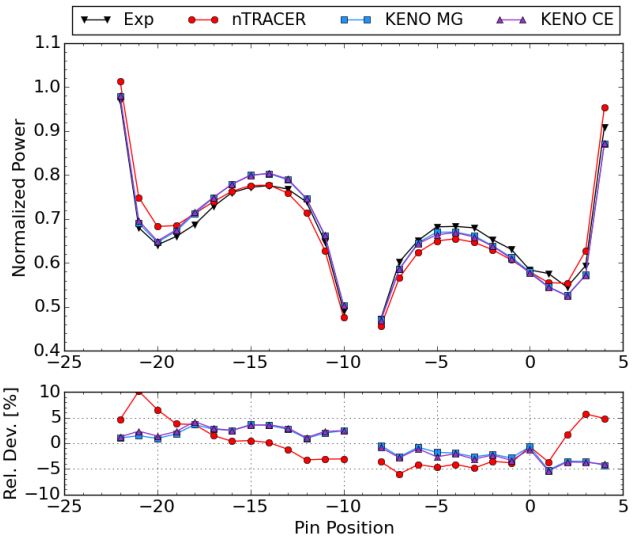

Fig. 5: Pin power distribution along the traverse of the VENUS-9/1 B_4C perturbation case, where seven pin positions are replaced by B_4C rods at position -9.

Fig. 5 shows the pin power distributions of the B_4C perturbation case. Compared to the nominal case, the substitution of the UO_2 rods by B_4C rods at position -9 causes larger deviations between the calculated and experimental pin powers. nTRACER underestimates the pin powers of the UO_2 rods by about -3% and the pin powers of the MOX rods by about -5%. The overestimation of the pin powers of the UO_2 rods by KENO increases up to -4% at position -14, -15 and up to -3% at position -10.

In Figure 6, the pin power distributions of the H_2O perturbation case are shown. The relative deviation between the pin powers calculated by KENO and the experimental values is increasing between the positions -20 to -15. At the positions around the perturbation, the KENO pin powers show a good agreement with the experiment. nTRACER underestimates the pin power of the UO_2 rod next to the perturbation by -7 %. nTRACER and KENO show a satisfying agreement with the experimental values for the pin powers of the MOX rods. The overestimation and underestimation, respectively, of nTRACER and KENO at the outer pin positions of the core remain the same.

The reason for the differences of the pin powers between the experimental values and nTRACER and KENO V.a may be the fact that simplifications in terms of geometry and material data are introduced in the models. Further investigations including the use of different nuclear data libraries and adjustments of the models and calculation parameters are planned.

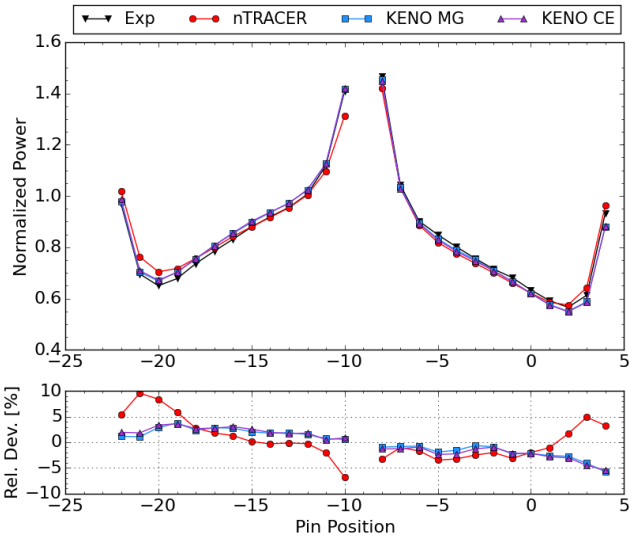

Fig. 6: Pin power distribution along the traverse of the VENUS-9/1 H_2O perturbation case, where seven pin positions are replaced by water cells at position -9.

IV. CONCLUSIONS

Neutron transport calculations of the VENUS-9/1 experiment are performed with the direct whole-core calculation code nTRACER and the Monte Carlo code KENO V.a of the SCALE 6.2 code package. The series of models includes the nominal case and three perturbation cases in which seven UO_2 4/0 fuel rods were replaced by either an Al-plate, B_4C rods or water cells.

In case KENO V.a is applied with the 238-group cross section library, nTRACER and KENO V.a show excellent agreement in terms of the multiplication factors for the nominal case and the three perturbation cases. The smallest difference, -8 pcm, is observed for the nominal case, while the B_4C case shows the largest difference with 91 pcm. KENO V.a in combination with continuous-energy cross section data calculates larger multiplication factors than nTRACER for all cases, and the reactivity differences are larger compared to KENO V.a in multi-group mode. Furthermore, the application of continuous-energy data leads to opposite results: the B_4C case shows the smallest difference with -15 pcm and for the nominal case, the largest difference of -105 pcm was obtained.

Furthermore, the pin power distribution obtained by nTRACER and KENO V.a for the demountable UO_2 and MOX fuel rods are compared to experimental values. For the nominal case and the three perturbation cases, the UO_2 and MOX pin powers calculated by nTRACER are in accordance with the experimental values. Discrepancies are only observed at the outer pin positions of the fissile regions. Here, the pin powers are overestimated by 5–10%. At the boundary between the fuel regions, nTRACER underestimates the pin powers; this is particularly visible for the H_2O perturbation case. KENO V.a in multi-group mode as well as in continuous-energy mode determines pin powers that are in good agreement with the experimental values for all cases. The pin powers of most of the UO_2 fuel rods are overestimated and an underestimation is observed for almost all MOX fuel rods. The largest discrepancy is observed at the outermost MOX fuel rod of the core, for which KENO V.a underestimates the pin power by -5 %. Further analyses are planned in order to figure out the reasons for those discrepancies. These intended studies should include a better adaptation of the models, the application of different nuclear data libraries and an adjustment of the calculation parameters.

Overall, the series of VENUS-9 and 9/1 configurations provide valuable experimental data for benchmark calculations with neutron transport codes. Therefore, studies of these configurations will be continued.

ACKNOWLEDGMENTS

This work is supported by the German Federal Ministry for Economic Affairs and Energy.

REFERENCES

1. "International Handbook of Evaluated Reactor Physics Benchmark Experiments," NEA/NSC/DOC(2006)1, NEA No. 7173, Organisation for Economic Co-operation and Development/Nuclear Energy Agency (2014).
2. L. LEENDERS, U. WEHMANN, C. GROVE, K. HESKETH, W. ZWERMANN, "IRPhEP Evaluation of VENUS 9 and VENUS 7 Experiments," *Nucl. Sci. Eng.*, **178**, 509-523 (2014).
3. Y.S. JUNG, C.B. SHIM, C.H. LIM, H.G. JOO, "Practical numerical reactor employing direct whole core neutron transport and subchannel thermal/hydraulic solvers," *Ann. Nucl. En.*, **62**, 357-374 (2013).
4. B.T. Rearden, M.A. JESSEE, "SCALE Code System," ORNL/TM-2005/39, Version 6.2, Oak Ridge, Tennessee (2016).
5. W. ZWERMANN, A. PAUTZ, S. MISU, W. TIMM, "VENUS-9, a Valuable Experimental Power Distribution Benchmark for Modern Transport Codes," *Proc. AMNT 2009*, Dresden, Germany, (2009) (CD-ROM).
6. W. ZWERMANN, S. LANGENBUCH, B.-C. NA, E. SARTORI, U.K. WEHMANN, "Summary of Results of the VENUS-7 Benchmark," *Proc. PHYSOR 2008*, Interlaken, Switzerland, Sep. 14-19, (2008) (CD-ROM).